Regular Article

PHYSICAL CHEMISTRY RESEARCH
Published by the
Iranian Chemical Society
www.physchemres.org
info@physchemres.org

Phys. Chem. Res., Vol. 7, No. 2, 245-259, June 2019
DOI: 10.22036/pcr.2019.153709.1554

Structural Investigation, Proton and Electron Affinities, Gas Phase Basicities, and Ionization Energies of Captopril

S. Naderi[a], H. Bahrami[a,*], M. Vahedpour[a] and M. Sabzehzari[b]

[a]*Department of Chemistry, University of Zanjan, P. O. Box: 38791-45371, Zanjan, Iran*

[b]*Department of Chemistry, Jundi-Shapur University of Technology, P. O. Box: 64615/334, Dezful, Iran*

(Received 25 October 2018, Accepted 24 January 2019)

Captopril is one of the most significant angiotensin-converting enzyme inhibitors. In spite of numerous experimental and computational studies on its properties, not enough geometrical and thermodynamic data are available on this compound. So, this study aimed to investigate the structural properties and assignment of possible conformers of captopril in the gas-phase. To this end, 1152 unique trial structures were generated by combinations of internal single-bond rotamers and pyrrolidine ring-inversion. A total of 119 conformers were found at the B3LYP/6-311++G** level after three sequential steps of optimization, and their relative energies, dipole moments, and rotational constants were obtained. The ionization energies, electron affinities, topical proton affinities, and gas-phase basicities of the first six low-energy conformers of captopril were also calculated *via* the abovementioned method. It is widely known that protonation is of great importance in the formation of new structures. Accordingly, the protonated forms of the favorable captopril conformers were structurally examined.

Keywords: Captopril, Conformational distribution, Topical proton affinity, Ionization energy

INTRODUCTION

Captopril, (2S)-1-[(2S)-2-methyl-3-sulfanylpropanoyl] pyrrolidine-2-carboxylic acid, is one of the most commonly used antihypertensive drugs in the world. It is widely accepted that captopril reduces blood pressure since it can function as a potent angiotensin-converting enzyme (ACE) inhibitor. Apart from its effect on treating blood pressure, captopril is able to perform other biological activities. There is a lot of evidence that cardiovascular and renal disease can be mitigated using captopril [1,2]. It has been proposed that captopril has the capability of inhibiting and reducing tumor growth. Its impact on the treatment of some cancers has also been reported in some studies [3,4]. Recently, it has been found that captopril is able to boost tumor blood perfusion and expand endothelial gaps in tumor blood vessels, and in this way, it can enhance tumor nanomedicine delivery [5]. The therapeutic impact of captopril on rheumatoid arthritis has also been substantiated [6,7].

The clinical and pharmacological significance of captopril is increasing in various fields of study over time. So, the research on various aspects of captopril properties has enjoyed numerous attention [8-10]. A majority of studies undertaken on captopril properties are related to the field of computational chemistry [11,12]. The flexibility of molecular structure of captopril is the primary reason for investigation of its conformational properties [13,14]. The studies carried out on the structure of captopril are mainly associated with its complexes including relevant enzymes [15]. A conformational analysis of captopril properties at the semiempirical AM1 level was conducted by Luke [16]. In his study, different values of six torsion angles were utilized to generate 216 initial conformations, which resulted in the formation of 123 unique structures of

*Corresponding author. E-mail: hbahrami@znu.ac.ir

captopril within 10.8 kcal mol^{-1} of the global minima. However, the starting sets of conformations chosen by Luke were limited; consequently, numerous possible rotamers were ignored and most likely some important local minima conformers were lost. Also, the conformations of the dianionic form of captopril by *Ab initio* calculations was reported by Zamarbide *et al*. [17]. Apart from the studies mentioned above, there is a dearth of research on the conformational distribution of captopril. Therefore, it is necessary to carry out a systematic theoretical study on captopril conformations by using an extensive set of trial conformers at an appropriate level of theory.

Proton transfer reactions are of paramount importance in the field of gas-phase ion chemistry, especially, atmospheric chemistry. Also, in biochemistry, proton transfer processes have vital roles in interactions, such as drug-enzyme interactions. Therefore, the investigation of proton transfer reactions has drawn numerous attention [18-21]. The possibility of proton transfer reactions is illustrated by proton affinity (PA) and gas-phase basicity (GB) [22]. Ionization energy (IE) and electron affinity (EA) are significant quantities in various areas of chemistry, for example, DNA and RNA bases [23], organic materials for electronics applications [24,25], and several types of drugs and drug-like chemicals [26,27].

The current study was designed to determine all possible gaseous captopril conformers and to gain more knowledge about the relative stability of different conformers and their conformational distribution at various temperatures. This study also examines the rotational constants and dipole moments of all the conformers. Besides, the thermodynamic quantities, including ionization energies, electron affinities, topical proton affinities, and gas-phase basicities, were measured for six low-energy conformers of captopril. Due to a dearth of knowledge on captopril chemical behavior, the results of the current study may contribute to the improvement of experimental and theoretical research and bioinformatics.

COMPUTATIONAL METHODS

The calculations were carried out using the Gaussian 09 program package. The Becke 3-parameter-Lee-Yang-Parr (B3LYP) hybrid functional [28] along with the split-valence triple-zeta basis sets, 6-311++G**, was used in all of the calculations. The study began with the conformational exploration of captopril. An initial set of trial conformers was built by the rotation of the five internal axes and also by the inversion of the pyrrolidine ring, as shown in Fig. 1. Trial structures were fully optimized in three different steps using the B3LYP method. The basis set was enhanced to a higher level in three steps. The unique conformers were selected to be further optimized at a higher level. The proton and electron affinities, gas-phase basicities, and ionization energies of the six low-energy conformers of captopril were calculated at the B3LYP/6-311++G** level of theory.

RESULTS AND DISCUSSION

Conformers and Energy

As depicted in Fig. 1, the initial set of trial conformers was built by the rotation of the five internal axes; *i.e.*, the C12-O3, C6-C12, C10-N, C10-C11, C11-C13 and, C13-S bonds, and also by the inversion of the pyrrolidine ring. Figure 1 indicates that rotamers include: (a) carboxyl groups with syn and anti conformations corresponding to 0° and 180° torsion angle, respectively, in respect of the OH functional group; (b) four different possibilities caused by the torsion around the C6-C12 bond, which are shown in Fig. 1 for four folds, -90°, 0°, 90°, 180°; (c) four possible rotamers about the C10-N amid bond; (d) three conformations constructed by varying the dihedral angles around the C10-C11 bond; (e) four different possibilities occurred by the torsion around the C11-C13 bond; (f) two rotamers allowed for the orientation of the -SH group. The inversion of pyrrolidine ring was defined by setting the two $C_7C_8C_9N$ dihedral angles at +30° and -30°.

In the first step, the trial structures were fully optimized at the B3LYP/3-21G level of theory and a set of 354 unique conformers was found. All of the obtained conformers were then subjected to further optimization at the B3LYP/6-311G* level and 202 unique conformers remained without any imaginary frequencies. Finally, the unique conformations were reoptimized at the B3LYP/6-311++G** level and a total of 119 unique conformations were located after three geometry optimizations. The optimized geometries in all steps were checked for their real frequencies.

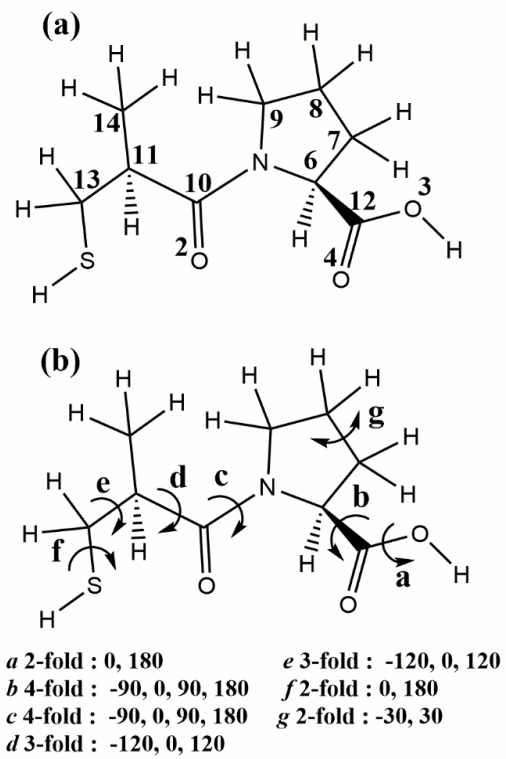

Fig. 1. (a) The sketch of the molecular structure of captopril, and (b) the illustration of the combination of internal rotamers resulting in various possible conformations.

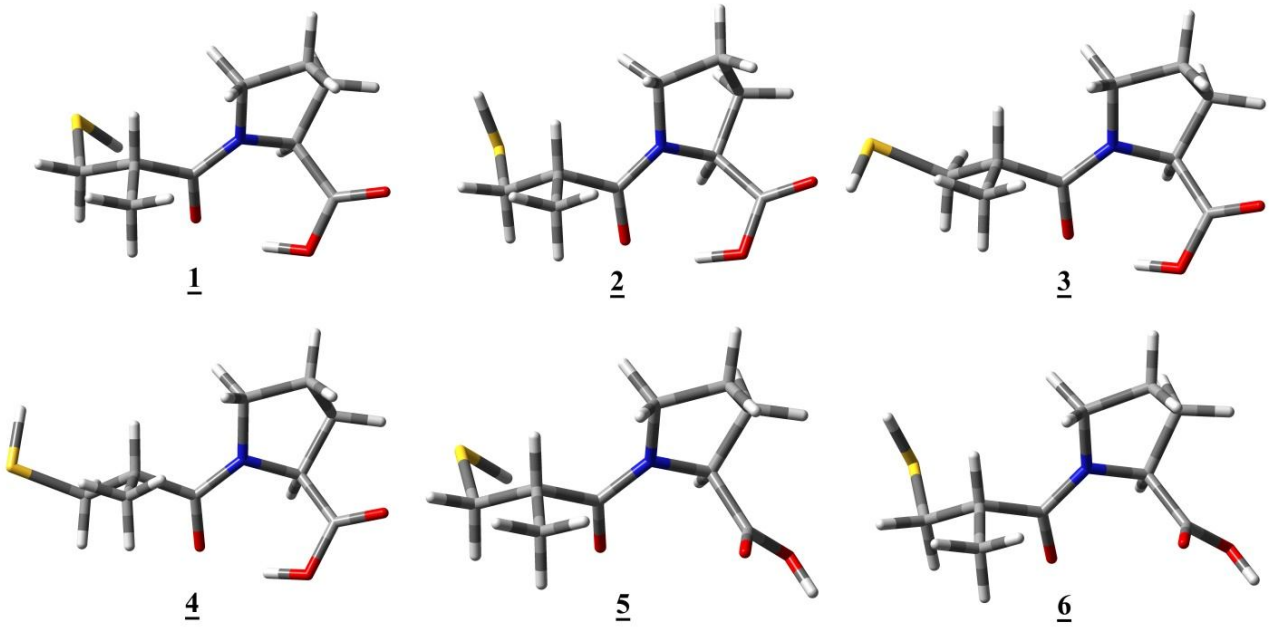

Fig. 2. The structures of the six low-energy *trans* conformers of captopril optimized at the B3LYP/6-311++G** level.

The structures of the six low-energy conformers of captopril are depicted in Fig. 2 and the Cartesian coordinates of all 119 unique conformers are provided in the Supplementary Material (S1). Table 1 shows the zero-point vibrational energies, relative energies, standard Gibbs free energies, rotational data, and dipole moments of all selected conformers. The relative total energy, including the zero-point vibrational energy and electronic energy, of the last stable conformer was estimated to be 57.3 kJ mol^{-1} at the B3LYP/6-311++G** level.

As saw in Fig. 2, all of the low-energy conformers of captopril were "trans" geometric isomers. The "*cis*" and "*trans*" isomers of captopril were interconverted by a rotation around the C-N amide bond [29]. The *cis*→*trans* isomerization barrier of captopril in the solution phase was calculated to be 89 kJ mol^{-1} through dynamic chromatography and electrophoresis [30]. The obtained value for this barrier of captopril is in a close agreement with that experimentally obtained using ^{13}C NMR band shape analysis and saturation transfer technics, [31]. It has already been reported that the bioactive form of the captopril is "*trans*" conformer [32]. The intramolecular hydrogen bond constructed between the carbonyl oxygen of amide group and the carboxylic acid hydrogen is one of the most contributing factors to the stability of *trans* isomer. Such hydrogen bonds were formed in four of the low-energy conformers obtained in this study. The calculations indicated that the 16th conformer with the relative energy of 15.21 kJ mol^{-1} is the first conformer with *cis* orientation.

Rotational Constants and Dipole Moments

It is widely known that the DFT predicts the rotational constants of conformers moderately accurate [33,34]. However, there is a dearth of experimental research on investigating the microwave spectra of gaseous captopril. Furthermore, rotational constants and dipole moments are considered as useful parameters providing a deeper understanding of conformational properties providing more knowledge for a more sound assignment of microwave spectra. Therefore, the rotational constants and dipole moments of the captopril conformers could be obtained at the B3LYP/6-311++G** level of theory, as presented in Table 1.

Conformational Distribution

The conformational distribution of the captopril conformers was computed *via* the Boltzmann distribution equation as follows:

$$\frac{N_i}{N_{total}} = \frac{e^{-E_{rel}/RT}}{\sum_{k=1}^{N_{total}} e^{-E_k/RT}} \quad (1)$$

The left side of the equation is the equilibrium ratio of conformer i over the sum of the total conformers. E_{rel} and E_k stand for the relative energy of the ith and kth conformers, respectively, in comparison with the minimum energy conformer [35]. The estimated conformational distributions at various temperatures are collected in Table 2.

Table 2 illustrates that the concentrations of conformer 1 and 2 were significantly high at all temperatures in comparison with that of other ones. At room temperature, the concentrations of conformer 1 and 2 were about 63% and 20%, respectively. Other conformers, including conformer 3, 4, and 5, might be detectable at room temperature. As the temperature increased, the diversity of the conformers in the gas-phase slowly shifted to the unstable conformers; so that, the ten low-energy conformers were the primary isomers at 500 K, accounting for over 80% of the distribution. Examining the conformational distribution of captopril at high temperature is of crucial importance because the operating temperature of some spectrometric techniques, such as ion mobility spectrometry, is up to 200 °C. Based on the results obtained here, it can be declared that captopril molecules at the cell temperature of 200 °C of the ion mobility spectrometer have as many diverse conformers as those in the gas phase. The obtained conformational results were in line with those expected in experimental research.

Topical Proton Affinities and Gas-phase Basicities

The PA is defined as the negative enthalpy (-ΔH) of the protonation of a molecule in the gas phase, and the GB refers to the negative Gibbs free energy change (ΔG) of the protonation reaction as shown in Eqs. (2) and (3), respectively.

$$M(g) + H^+(g) \rightarrow MH^+ \quad PA = -\Delta H \quad (2)$$

Table 1. The Zero-point Vibrational Energies, Relative Energies, Relative Standard Gibbs Free Energies, Rotational Parameters, and Dipole Moments of the Gaseous Captopril Conformers

Conformer			Relative energies (kJ mol^{-1})		Rotational constants (GHz)			Dipole (D)
		ZPVE	ΔE_{tot}	ΔG^o	A	B	C	
1	*trans*	627.00	0.00	0.00	0.966	0.374	0.345	5.10
2	*trans*	627.00	2.81	0.01	0.952	0.386	0.342	6.39
3	*trans*	626.59	6.61	2.55	1.220	0.309	0.275	4.80
4	*trans*	626.46	6.65	3.31	1.225	0.309	0.275	5.88
5	*trans*	625.45	7.11	1.69	0.973	0.357	0.345	3.93
6	*trans*	624.91	10.99	4.14	0.964	0.363	0.342	4.26
7	*trans*	625.28	11.21	4.83	0.971	0.362	0.348	5.10
8	*trans*	626.87	11.45	8.92	1.122	0.351	0.302	6.55
9	*trans*	625.94	11.90	7.95	1.160	0.312	0.274	6.10
10		626.86	12.43	9.05	1.079	0.352	0.314	6.07
11	*trans*	626.59	12.74	8.30	1.111	0.333	0.276	5.08
12	*trans*	624.60	13.56	5.89	1.207	0.305	0.279	3.97
13	*trans*	626.10	13.64	7.99	1.116	0.331	0.275	5.87
14	*trans*	624.60	13.80	6.75	1.206	0.306	0.279	5.02
15	*trans*	624.59	14.89	6.41	0.959	0.372	0.343	5.86
16	*cis*	624.98	15.21	8.86	0.817	0.452	0.396	3.58
17	*cis*	624.77	15.76	9.12	0.810	0.444	0.384	5.21
18	*trans*	626.10	16.31	10.49	1.106	0.337	0.278	5.92
19	*trans*	624.31	16.88	8.50	1.208	0.307	0.281	3.80
20	*trans*	625.24	17.45	11.93	1.063	0.354	0.309	5.76
21	*cis*	624.87	17.68	11.21	0.868	0.426	0.332	4.69
22	*trans*	626.84	17.75	14.53	1.001	0.369	0.319	6.13
23	*cis*	624.38	17.75	9.29	0.898	0.392	0.320	5.59
24	*trans*	624.74	17.77	10.97	1.209	0.307	0.282	5.43
25	*trans*	624.81	17.82	10.55	1.209	0.307	0.281	4.68

Table 1. Continued

26	*trans*	624.65	17.88	9.28	1.092	0.326	0.280	4.90
27	*trans*	624.34	19.37	12.92	1.121	0.319	0.282	5.54
28	*trans*	624.61	19.54	12.20	1.090	0.334	0.283	4.17
29	*cis*	625.38	19.90	14.03	0.794	0.483	0.398	3.81
30	*cis*	624.34	20.16	13.16	0.870	0.422	0.326	5.84
31	*trans*	625.94	20.20	16.67	1.105	0.361	0.307	7.53
32	*trans*	624.46	20.57	11.52	1.096	0.328	0.282	5.56
33	*cis*	624.60	20.79	13.03	0.914	0.388	0.322	4.12
34	*trans*	626.50	21.19	18.16	0.956	0.396	0.337	6.38
35	*trans*	625.31	21.20	15.82	1.071	0.356	0.312	6.28
36	*cis*	624.51	21.36	12.31	0.908	0.391	0.322	3.15
37	*cis*	624.57	21.47	13.95	0.869	0.429	0.334	4.63
38	*cis*	624.25	21.53	14.58	0.797	0.447	0.385	5.69
39	*cis*	625.15	21.93	19.21	0.814	0.461	0.398	3.47
40	*cis*	625.19	22.14	18.57	0.802	0.463	0.392	3.11
41	*cis*	625.25	22.20	16.70	1.036	0.363	0.317	6.27
42	*cis*	624.60	23.15	15.18	0.886	0.415	0.329	4.35
43	*trans*	625.24	23.40	17.11	0.998	0.357	0.335	5.89
44	*trans*	624.65	23.74	17.74	0.979	0.381	0.345	3.73
45	*trans*	625.09	23.81	17.21	0.961	0.371	0.328	6.31
46	*cis*	624.59	23.87	16.35	0.885	0.413	0.327	3.30
47	*trans*	627.16	24.07	21.23	1.044	0.338	0.303	5.56
48	*cis*	625.50	24.64	18.68	1.038	0.364	0.321	4.60
49	*trans*	626.97	24.77	22.90	0.842	0.427	0.401	7.16
50	*trans*	628.34	25.66	25.31	0.870	0.439	0.400	6.21
51	*trans*	627.12	25.71	23.37	1.046	0.338	0.302	6.72
52	*trans*	626.81	25.97	22.66	1.000	0.337	0.302	5.61
53	*trans*	624.85	26.20	20.16	0.977	0.378	0.332	7.09
54	*trans*	627.08	26.68	24.49	0.839	0.426	0.391	7.16

Table 1. Continued

55	*cis*	625.24	27.10	21.72	0.975	0.380	0.324	4.77
56	*trans*	626.71	27.24	24.14	0.792	0.453	0.389	7.53
57	*trans*	624.33	27.78	21.41	0.979	0.383	0.348	5.55
58	*trans*	624.28	28.12	21.34	1.048	0.362	0.313	5.43
59	*trans*	627.30	28.43	26.89	0.871	0.459	0.425	3.60
60	*trans*	627.65	28.47	27.44	0.877	0.424	0.391	7.43
61	*cis*	624.85	29.24	23.39	0.909	0.379	0.314	3.63
62	*trans*	624.43	29.94	23.54	1.269	0.295	0.274	6.42
63	*trans*	624.47	30.18	23.24	1.267	0.295	0.274	5.58
64	*trans*	626.23	30.37	26.12	0.817	0.471	0.396	5.34
65	*trans*	624.34	30.64	21.18	1.225	0.304	0.274	5.29
66	*trans*	624.84	30.93	24.84	1.038	0.343	0.311	5.22
67	*cis*	625.17	31.44	26.33	0.915	0.374	0.312	4.18
68	*trans*	624.24	31.71	24.73	1.058	0.363	0.315	6.58
69	*cis*	624.58	32.29	26.47	0.879	0.400	0.322	4.39
70	*cis*	624.17	32.72	25.27	1.048	0.364	0.319	6.09
71	*trans*	625.35	33.32	29.25	1.114	0.338	0.302	7.18
72	*trans*	624.87	33.46	27.45	1.040	0.344	0.313	4.39
73	*trans*	627.63	33.94	30.59	0.837	0.443	0.389	6.34
74	*cis*	624.50	34.11	27.37	0.872	0.422	0.359	5.68
75	*cis*	625.81	34.46	30.95	1.048	0.357	0.315	3.56
76	*trans*	626.86	34.62	32.30	0.879	0.451	0.418	4.21
77	*cis*	624.32	34.79	26.25	1.048	0.366	0.323	3.91
78	*cis*	624.15	35.10	26.95	0.827	0.474	0.387	3.18
79	*trans*	624.54	35.48	28.41	1.090	0.335	0.315	6.63
80	*trans*	625.15	35.52	30.06	1.042	0.344	0.313	5.78
81	*trans*	625.89	36.19	30.37	0.837	0.450	0.400	5.44
82	*trans*	625.72	36.60	32.05	0.892	0.422	0.400	3.92
83	*trans*	624.80	36.67	30.54	0.850	0.424	0.400	4.08

Table 1. Continued

84	*trans*	627.41	36.97	34.34	0.843	0.427	0.384	7.55
85	*trans*	625.09	37.26	32.26	0.807	0.446	0.395	5.22
86	*trans*	624.78	38.55	32.12	0.851	0.431	0.401	4.95
87	*trans*	625.60	38.65	34.89	0.847	0.466	0.400	7.74
88	*cis*	626.00	38.81	35.28	0.787	0.469	0.422	3.25
89	*cis*	625.19	38.85	35.87	0.833	0.488	0.395	3.51
90	*cis*	626.06	39.39	36.31	0.768	0.476	0.423	3.90
91	*trans*	625.89	39.55	35.21	0.892	0.428	0.405	5.19
92	*cis*	625.33	39.73	35.17	0.872	0.391	0.333	5.33
93	*cis*	624.66	39.73	33.42	0.804	0.457	0.407	4.10
94	*cis*	625.16	40.35	35.09	0.888	0.386	0.335	2.84
95	*trans*	623.69	40.80	31.67	0.993	0.379	0.343	6.90
96	*cis*	625.14	40.83	36.13	0.901	0.413	0.357	5.31
97	*cis*	625.20	41.55	36.51	0.883	0.389	0.335	3.79
98	*cis*	625.85	41.87	37.79	0.778	0.472	0.426	2.01
99	*cis*	625.58	41.97	37.28	0.735	0.491	0.451	2.59
100	*trans*	624.39	42.11	36.46	1.102	0.344	0.306	8.08
101	*cis*	625.18	43.10	37.91	0.905	0.414	0.360	3.78
102	*cis*	623.28	43.51	36.26	0.870	0.427	0.329	7.04
103	*cis*	624.83	43.93	38.49	1.051	0.360	0.318	2.44
104	*cis*	623.27	44.62	37.70	0.873	0.423	0.327	6.61
105	*cis*	625.72	45.74	41.44	0.687	0.515	0.465	2.51
106	*cis*	623.03	46.32	39.46	0.799	0.447	0.388	6.98
107	*trans*	626.82	48.28	46.47	0.885	0.457	0.400	8.19
108	*cis*	626.33	48.78	46.44	0.784	0.468	0.425	1.54
109	*cis*	625.43	48.92	44.26	0.801	0.463	0.417	1.57
110	*cis*	625.50	49.06	45.25	0.879	0.384	0.334	2.99
111	*cis*	626.10	49.18	46.28	0.805	0.461	0.420	2.42
112	*cis*	625.52	50.04	46.59	0.875	0.386	0.334	2.46

Table 1. Continued

113	*cis*	623.92	50.05	43.69	0.944	0.395	0.329	7.75
114	*cis*	625.29	51.59	46.95	0.784	0.513	0.353	3.40
115	*cis*	625.29	51.91	48.04	0.908	0.408	0.358	1.73
116	*cis*	625.98	55.04	52.00	0.677	0.518	0.471	2.06
117	*cis*	625.46	56.13	51.48	0.818	0.399	0.343	3.43
118	*cis*	626.74	56.54	53.57	0.741	0.486	0.438	1.66
119	*cis*	626.51	57.33	53.84	0.763	0.479	0.430	2.64

Table 2. The Conformational Distribution (Percentage) of the Gaseous Captopril Conformers at Various Temperatures

Conformer	198 K	273 K	298 K	398 K	498 K
1	80.9	67.0	62.5	46.5	34.3
2	14.6	19.4	20.0	19.8	17.4
3	1.5	3.6	4.3	6.3	7.0
4	1.4	3.5	4.2	6.2	6.9
5	1.0	2.9	3.5	5.4	6.2
6	0.1	0.6	0.7	1.7	2.4
7	-	0.5	0.7	1.6	2.3
8	-	0.4	0.6	1.5	2.2
9	-	0.3	0.5	1.3	1.9
10	-	0.3	0.4	1.1	1.7
11	-	0.2	0.3	1.0	1.6
12	-	0.2	0.3	0.8	1.3
13	-	0.2	0.2	0.7	1.3
14	-	0.1	0.2	0.7	1.2
15	-	-	0.1	0.5	0.9

$$GB = -\Delta G \quad (3)$$

However, the PA of a molecule obtained from the experimental methods is usually corresponding to the protonation at the most basic sites of that molecule. While the PA of a multifunctional molecule protonated at a less basic site is difficult to obtain *via* the experimental methods, several PA values, called topical proton affinities (TPA), can be achieved using the computational methods. Several values of topical gas-phase basicities (TGB) can be calculated through the same process.

The main impetus for focusing on TPA and TGB is that they facilitate the examination of ion-molecule reactions for the purpose of generating new ion structures which might be observed in different spectrometric methods, such as ion mobility spectrometry, or in various atmospheric conditions. The experimental methods, such as mass spectrometry, used to investigate proton transfer reactions to molecular species cannot provide sufficient information on where protons are attached. In this regard, the density functional theory can be utilized to reveal specifically which one of the possible protonated analogs leads to the PA value.

The TPA and TGB of the six low-energy conformers of captopril were calculated through Eqs. (2) and (3), where M stood for each conformer. All of the six conformers were protonated *via* five sites, including one nitrogen (N), three oxygen atoms, (O2, O3, O4) and one sulfur (S) atom, as displayed in Fig. 1. The Cartesian coordinates for the output structures of all 30 protonated captopril isomers are presented in the Supplementary Material (S2). Considering the proton as a classical particle, the enthalpy and Gibbs free energies of the proton at 298.15 K were equal to 6.20 kJ mol^{-1} and -26.28 kJ mol^{-1}, respectively [36]. The TPAs and TGBs of the conformers, determined for different protonation sites at the B3LYP/6-311++G** level of computation, are exhibited in Table 3.

As shown in Table 3, for all of the molecules, the O2 site (the oxygen atom of the amide group) was the preferred site for protonation. In Table 4, the values of TPAs and TGBs are reported by one and double stars signifying the attachment of the proton to some sites. In some cases, after the optimization of MH^+, the chemical nature of the protonated molecules changed. So, the TPA and TGB of the mentioned species in the corresponding protonation sites are meaningless, and as a result, no data could be reported for them. The changing chemical nature of the protonated captopril pertained to two paths. The first path was the proton transfer from the specific protonation site to the next desirable site and the obtained isomer was more stable than the expected isomer. The second path was the elimination of the water molecule from MH^+ accompanied by the formation of a positively charged fragment ion. Also, in this path, the obtained species were more stable than the corresponding MH^+ isomer. The water molecule was removed from conformer 5 and 6 by the protonation of the O3 site (the hydroxyl oxygen of the carbocyclic acid group) and the five-membered ring structure remained. The pathway of the water molecule elimination is shown in Fig. 3. The formation of cyclic ionic compounds due to the elimination of the water molecule during protonation has been reported for some molecules before [37].

Ionization Energy and Electron Affinity

The energy difference between a neutral molecule and its cation or anion states when all species are in their ground electronic states and gas phase are called adiabatic ionization energy (AIE) and adiabatic electron affinity (AEA), respectively. On the other hand, the vertical ionization energy (VIE) and the vertical electron affinity (VEA) are defined as the electronic energy difference between the ground states of a neutral molecule and its anion or cation at the equilibrium geometry of neutral molecules [37-39].

The B3LYP method was used to estimate both vertical and adiabatic ionization energies of the six low-energy conformers of captopril. The obtained AIE and VIE energies are shown in Table 4.

Comparing the AIE and VIE values revealed that in general, the VIE values were greater than the AIE values, which can be attributed to the optimized geometry of the captopril in an ionic form used in the AIE calculation. The IEs almost remained the same in the first four stable conformers while the AIEs of conformer 5 and 6 decreased about 50 kJ mol^{-1} and their VIEs dropped about 20 kJ mol^{-1}. Due to the weakness of intramolecular hydrogen bond, conformer 5 and 6 were relatively less stable in their neutral form.

The adiabatic and vertical electron affinities of the six

Table 3. The Calculated Topical Proton Affinities and Gas-phase Basicities at 298.15 K for the Selected Conformers of Captopril (kJ mol^{-1})

Conformer	TPA					TGB				
	N	O2	O3	O4	S	N	O2	O3	O4	S
1	839.69	915.31	*	*	802.46	813.62	884.33	*	*	769.71
2	843.764	920.94	*	*	*	818.03	888.28	*	*	*
3	835.98	913.68	*	*	779.54	809.65	881.25	*	*	748.28
4	835.25	912.98	*	*	779.51	809.56	880.85	*	*	749.88
5	878.48	923.43	**	861.07	837.70	848.32	888.49	**	827.25	805.27
6	883.49	918.60	**	867.75	832.17	851.54	885.03	**	831.18	799.20

*The migration of added proton to the O atom number 2. **The elimination of H_2O and ring formation.

Table 4. The Calculated Adiabatic (AIE) and Vertical Ionization Energies (VIE) (kJ mol^{-1}) of the Six Low-energy Conformers of Captopril

Conformer	AIE	VIE
1	832.09	848.27
2	826.83	847.56
3	827.27	843.40
4	827.44	843.78
5	773.72	822.29
6	769.38	822.18

low-energy conformers of captopril were computed at the B3LYP level of theory using the 6-311++G** basis set. The calculated VEA and AEA values are presented in Table 5. The results indicated that the VEA values were more positive in comparison with those of the AEA. However, in general, the EA values were low and close to zero. The AEA values for some of the conformers (conformer 3 and 4) were negative. The observed trend of the obtained AEA values suggests that the negative ion associated with some captopril conformers is more stable than that related to the neutral conformers.

CONCLUSIONS

Using comprehensive trial structures of the gas-phase captopril molecule, up to 119 unique conformers were found at the B3LYP/6-311++G** level through geometry optimization and the calculations of vibrational frequencies. The rotational constants, dipole moments, and conformational distributions at various temperatures were

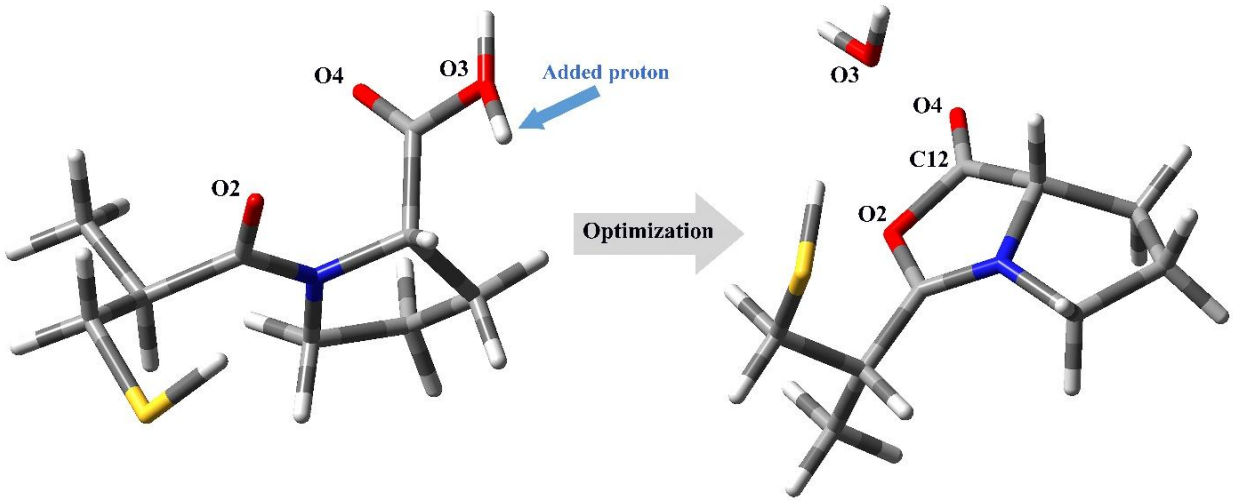

Fig. 3. The removal of the H_2O molecule after the optimization of the protonated captopril (conformer 5).

Table 5. The Calculated Adiabatic (AEA) and Vertical Electron Affinities (VEA) (kJ mol^{-1}) of the Six Low-energy Conformers of Captopril

Conformer	AEA	VEA
1	-9.18	-16.35
2	-0.07	-8.80
3	14.76	-10.99
4	9.95	-2.87
5	-18.37	-25.56
6	-15.12	-22.36

reported. The topical proton affinities, gas-phase basicities, and adiabatic and vertical ionization energies of the six low-energy conformers of captopril were calculated. The oxygen atom of the carbonyl functional group was the most favorable site for protonation. The topical proton affinities of the six stable conformers for the protonation of this site were estimated to be in the range of 912.98-923.43 kJ mol^{-1}. The estimated topical gas-phase basicities of the six stable conformers were approximately the same. Their numerical values were in the range of 880.65-888.49 kJ mol^{-1}. The vertical ionization energy values were more than the values of adiabatic ionization energies. The calculated electron affinities were approximately the same and their values were near zero.

ACKNOWLEDGMENTS

The authors are highly grateful to University of Zanjan, for its financial support.

REFERENCES

[1] Salah, E. M.; Bastacky, S. I.; Jackson, E. K.; Tofovic, S. P., Captopril attenuates cardiovascular and renal disease in a rat model of heart failure with preserved ejection fraction. *J. Cardiovasc. Pharmacol.* **2018**, *71*, 205-214, DOI: 10.1097/FJC.0000000000000561.

[2] Li, T.; Zhou, R.; Yao, Y.; Yang, Q.; Zhou, C.; Wu, W.; Li, Q.; You, Z.; Zhao, X.; Yang, L.; Li, C.; Zhu, D.; Qiu, Y.; Luo, M.; Tan, Z.; Li, H.; Chen, Y.; Gong, G.; Feng, Y.; Dian, K.; Liu, J., Angiotensin-converting enzyme inhibitor captopril reverses the adverse cardiovascular effects of polymerized hemoglobin. *Antioxid. Redox Signal.* **2014**, *21*, 2095-2108, DOI: 10.1089/ars.2013.5606.

[3] Attoub, S.; Gaben, A. M.; Al-Salam, S.; Al Sultan, M. A. H.; John, A.; Nicholls, M. G.; Mester, J.; Petroianu, G., Captopril as a potential inhibitor of lung tumor growth and metastasis. *Ann. N.Y. Acad. Sci.* **2008**, 1138, 65-72, DOI: 10.1196/annals.1414.011.

[4] Nakaya, K.; Otsuka, H.; Kondo, K.; Otani, T.; Nagata, M., Tumor growth-inhibitory effect of an angiotensin-converting enzyme inhibitor (captopril) in a lung cancer xenograftmodel analyzed using 18F-FDG-PET/CT. *Nucl. Med. Commun.* **2016**, *37*, 139-146, DOI: 10.1097/MNM.0000000000000404.

[5] Zhang, B.; Jiang, T.; Tuo, Y.; Jin, K.; Luo, Z.; Shi, W.; Mei, H.; Hu, Y.; Pang, Z.; Jiang, X., Captopril improves tumor nanomedicine delivery by increasing tumor blood perfusion and enlarging endothelial gaps in tumor blood vessels. *Cancer Lett.* **2017**, *410*, 12-19, DOI: 10.1016/j.canlet.2017.09.007.

[6] Liu, H. -M.; Wang, K. -J., Therapeutic effect of captopril on rheumatoid arthritis in rats. *Asian. Pac. J. Trop. Med.* **2014**, *7*, 996-999, DOI: 10.1016/S1995-7645(14)60175-9.

[7] Popa, C. D.; van Riel, P. L. C. M., The use of captopril in rheumatoid arthritis: Combining treatment targets! *Can. J. Cardiol.* **2013**, *29*, 639.e13, DOI: 10.1016/j.cjca.2013.02.017.

[8] Ala, S.; Enayatifard, R.; Alvandipour, M.; Qobadighadikolaei, R., Comparison of captopril (0.5%) cream with diltiazem (2%) cream for chronic anal fissure: a prospective randomized double-blind two-centre clinical trial. *Colorectal Dis.* **2016**, *18*, 510-516, DOI: 10.1111/codi.13147.

[9] Small Jr, W.; James, J. L.; Moore, T. D.; Fintel, D. J.; Lutz, S. T.; Movsas, B.; Suntharalingam, M.; Garces, Y. I.; Ivker, R.; Moulder, J., Utility of the ACE inhibitor captopril in mitigating radiation-associated pulmonary toxicity in lung cancer: results from NRG oncology RTOG 0123. *Am. J. Clin. Oncol.* **2016**, DOI: 10.1097/COC.0000000000000289.

[10] Meng, X.; Li, Y.; Wang, X.; Li, J.; Liu, Y.; Yu, Y., Evaluation of the saline infusion test and the captopril challenge test in chinese patients with primary aldosteronism. *J. Clin. Endocrinol. Metab.* **2017**, *103*, 853-860, DOI: 10.1210/jc.2017-01530.

[11] Berger, G.; Chab-Majdalani, I.; Hanessian, S., Properties of the amide bond involving proline 4,5-methanologues: An experimental and theoretical study. *Isr. J. Chem.* **2017**, *57*, 1-12, DOI: 10.1002/ijch.201600106.

[12] de Souza, M. C.; Diniz, L. F.; de Jesus Franco, C. H.; de Abreu, H. A.; Diniz, R., Structural study of the stability of the captopril drug regarding the formation of its captopril disulphide dimer. *J. Struct. Chem.* **2016**, *57*, 1111-1120, DOI: 10.1134/S0022476616060081.

[13] Andrews, P. R.; Carson, J. M.; Caselli, A.; Spark, M. J.; Woods, R., Conformational analysis and active site modeling of angiotensin-converting enzyme inhibitors. *J. Med. Chem.* **1985**, *28*, 393–399, DOI: 10.1021/jm00381a021.

[14] Thorsett, E. D.; Harris, E. E.; Aster, S. D.; Peterson, E. R.; Snyder, J. P.; Springer, J. P.; Hirshfield, J.; Tristram, E. W.; Patchett, A. A., Conformationally restricted inhibitors of angiotensin-converting enzyme. Synthesis and computations. *J. Med. Chem.* **1986**, *29*, 251-260, DOI: 10.1021/jm00152a014.

[15] Natesh, R.; Schwager, S. L. U.; Evans, H. R.; Sturrock, E. D.; Acharya, K. R., Structural details on the binding of antihypertensive drugs captopril and enalaprilat to human testicular angiotensin I-converting enzyme. *Biochemistry.* **2004**, *43*, 8718-8724, DOI: 10.1021/bi049480n.

[16] Luke, B. T., A quantum mechanical conformational

search of captopril, a potent inhibitor of the angiotensin-converting enzyme. *J. Mol. Strut.* **1994**, *309*, 1-11, DOI: 10.1016/0166-1280(94)80055-3.

[17] Zamarbide, G. N., Estrada, M. R., Zamora, M. A., Torday, L. L., Enriz, R. D., Vert, F. T., Csizmadia, I. G., An *ab initio* conformational study on captopril. *J. Mol. Struct. (THEOCHEM)* **2003**, *666-667*, 599-608, DOI: 10.1016/j.theochem.2003.08.084.

[18] Salpin, J. -Y.; Haldys, V.; Steinmetz, V.; Léon, E.; Yáñez, M.; Montero-Campillo, M. M., Protonation of methyluracils in the gas phase: The particular case of 3-methyluracil. *Int. J. Mass Spectrom.* **2018**, *429*, 47-55, DOI: 10.1016/j.ijms.2017.05.004.

[19] Valadbeigi, Y., Proton affinities and gas phase basicities of epoxides and episulfides: Exceptional superbasicity of compounds with oxygen and sulfur sites. *Int. J. Mass Spectrom.* **2018**, *431*, 63-69, DOI: 10.1016/j.ijms.2018.06.007.

[20] Kabanda, M. M.; Ebanos, E. E., DFT study of the protonation and deprotonation enthalpies of benzoxazole, 1,2-benzisoxazole and 2,1-benzisoxazole and implications for the structures and energies of their adducts with explicit water molecules. *J. Theory. Comput Chem.* **2013**, *12*, 1350070, DOI: 10.1142/S0219633613500703.

[21] Safi, Z. S.; Hasanat, S. J. A.; Wazzan, N. A., DFT investigation of the amino/imino proton transfer process of 2-amino-2-oxazolin-4-one in gas phase and solution. *J. Theor. Comput Chem.* **2018**, *17*, 1850004, DOI: 10.1142/S0219633618500049.

[22] Valadbeigi, Y., A mathematic model for proton affinity of organic molecules: Effect of size, chain length and nature of surrounding groups on the proton affinity of a site. *Int. J. Mass Spectrom.* **2016**, *395*, 49-52, DOI: 10.1016/j.ijms.2015.12.002.

[23] Crespo-Hernández, C. E.; Arce, R.; Ishikawa, Y.; Gorb, L.; Leszczynski, J.; Close, D. M., *Ab initio* ionization energy thresholds of DNA and RNA bases in gas phase and in aqueous solution. *J. Phys. Chem. A* **2004**, *108*, 6373-6377, DOI: 10.1021/jp049270k.

[24] Richard, R. M.; Marshall, M. S.; Dolgounitcheva, O.; Ortiz, J. V.; Brédas, J.-L.; Marom, N.; Sherrill, C. D., Accurate ionization potentials and electron affinities of acceptor molecules I. Reference data at the CCSD(T) complete basis set limit. *J. Chem. Theory Comput.* **2016**, *12*, 595-604, DOI: 10.1021/acs.jctc.5b00875.

[25] Zheng, C.; Rubel, O., Ionization energy as a stability criterion for halide perovskites. *J. Phys. Chem. C* **2017**, *121*, 11977-11984, DOI: 10.1021/acs.jpcc.7b00333.

[26] Liu, H.; Ding, Y.; Walker, L. A.; Doerksen, R. J., Computational study on the effect of exocyclic substituents on the ionization potential of primaquine: insights into the design of primaquine-based antimalarial drugs with less methemoglobin generation. *Chem. Res. Toxicol.* **2015**, *28*, 169-174.

[27] Bensasson, R. V.; Dinkova-Kostova, A. T.; Zheng, S.; Saito, A.; Li, W.; Zoete, V.; Honda, T., Electron affinity of tricyclic, bicyclic, and monocyclic compounds containing cyanoenones correlates with their potency as inducers of a cytoprotective enzyme. *Bioorg. Med. Chem. Lett.* **2016**, *26*, 4345-4349, DOI: 10.1016/j.bmcl.2016.07.028.

[28] Becke, A. D., Density□functional thermochemistry. III. The role of exact exchange. *J. Chem. Phys.* **1993**, *98*, 5648-5652, DOI: 10.1063/1.464913.

[29] Shun-Li, W.; Shan-Yang, L.; Ting-Fang, C.; Chi-Hsiang, C., Solid-state *trans-cis* isomerization of captopril determined by thermal fourier transform infrared (FT-IR) microspectroscopy. *J. Pharm. Sci.* **2001**, *90*, 1034-1039.

[30] Oliver, T., Direct calculation of interconversion barriers in dynamic chromatography and electrophoresis: Isomerization of captopril. *Electrophoresis.* **2005**, *26*, 487-493, DOI: 10.1002/elps.200410235.

[31] Green, D. V. S.; Hillier, I. H.; Morris, G. A.; Whalley, L., Determination of the barrier to C-N bond rotation in captopril: Application of reference deconvolution to line-shape analysis. *Magn. Reson. Chem.* **1990**, *28*, 820-823, DOI: 10.1002/mrc.1260280916.

[32] Tzakos, A. G.; Naqvi, N.; Comporozos, K.; Pierattelli, R.; Theodorou, V.; Husain, A.; Gerothanassis, I. P., The molecular basis for the selection of captopril cis and trans conformations by angiotensin I converting enzyme. *Bioorg. Med. Chem. Lett.* **2006**, *16*, 5084-5087, DOI: 10.1016/j.bmcl.2006.07.034.

[33] Sheng, Y.; Venkatraman, R.; Kwiatkowski, J. S.; Majewska, J.; Leszczynski, J., A DFT and MP2 study on the molecular structure and vibrational spectra of halogenosubstituted phosphoryl and thiophosphoryl compounds. *Struct. Chem*. **2003**, *14*, 511-525, DOI: 10.1023/B:STUC.0000004495.57863.63

[34] Marstokk, K. M.; Møllendal, H.; Samdal, S., Microwave spectrum, conformational equilibrium, 14N quadrupole coupling constants, dipole moment, vibrational frequencies and quantum chemical calculations for acrylamide. *J. Mol. Struct.* **2000**, *524*, 69-85, DOI: 10.1016/S0022-2860(99)00362-2.

[35] Contributors, W. Conformational isomerism --- {Wikipedia}{,} The Free Encyclopedia. https://en.wikipedia.org/w/index.php?title=Conformational_isomerism&oldid=844785533.

[36] Fifen, J. J.; Dhaouadi, Z.; Nsangou, M., Revision of the thermodynamics of the proton in gas phase. *J. Phys. Chem.* **2014**, *118*, 11090-11097. DOI: 10.1021/jp508968z.

[37] Valadbeigi, Y.; Farrokhpour, H.; Tabrizchi, M., G4MP2, DFT and CBS-Q calculation of proton and, electron affinities, gas phase basicities and ionization energies of hydroxylamines and alkanolamines. *J. Chem. Sci.* **2014**, *126*, 1209-1215, DOI: 10.1007/s12039-014-0668-y.

[38] Rienstra-Kiracofe, J. C.; Tschumper, G. S.; Schaefer, H. F.; Nandi, S.; Ellison, G. B., Atomic and molecular electron affinities: Photoelectron experiments and theoretical computations. *Chem. Rev.* **2002**, *102*, 231-282. DOI: 10.1021/cr990044u.

[39] Farajmand, B.; Bahrami, H., Electron ionization of serine and threonine: A discussion about peak intensities. *Phys. Chem. Res.* **2016**, *4*, 539-551, DOI: 10.22036/pcr.2016.15560.